

This discussion paper is/has been under review for the journal Atmospheric Chemistry and Physics (ACP). Please refer to the corresponding final paper in ACP if available.

Acetylene C₂H₂ retrievals from MIPAS data and regions of enhanced upper tropospheric concentrations in August 2003

R. J. Parker, J. J. Remedios, D. P. Moore, and V. P. Kanawade

Earth Observation Science, Space Research Centre, University of Leicester, UK

Received: 11 August 2010 – Accepted: 22 November 2010 – Published: 7 December 2010

Correspondence to: R. J. Parker (rjp23@le.ac.uk)

Published by Copernicus Publications on behalf of the European Geosciences Union.

MIPAS retrievals Of acetylene

R. J. Parker et al.

Title Page

Abstract

Introduction

Conclusions

References

Tables

Figures

◀

▶

◀

▶

Back

Close

Full Screen / Esc

Printer-friendly Version

Interactive Discussion



Abstract

Acetylene (C_2H_2) volume mixing ratios (VMRs) have been successfully retrieved from MIPAS Level 1B radiances during August 2003. The data presented here contain most information between 300 hPa and 100 hPa based on the averaging kernels, with information also at lower altitude levels (up to 500 hPa) albeit with some influence from the 300 hPa level. In our C_2H_2 retrievals, data at altitude levels above 100 hPa must be treated with caution. Systematic errors are less than 10% at the upper levels but can reach higher levels at 300 hPa in the tropics due to water vapour influences. Random errors per point are less than 15% at lower pressure levels and are closer to 30% at 100 hPa.

Global distributions of both the absolute C_2H_2 and ratios to MOPITT 150 hPa retrievals of carbon monoxide (CO) confirm some significant features for this important hydrocarbon in a characteristic summer month (August 2003), showing tight correlations regionally but globally emphasising the differences between sources and lifetimes of CO and C_2H_2 . The ratios to CO are estimated to be accurate to approximately 10%. A strong isolation of C_2H_2 within the Asian monsoon anticyclone is observed, evidencing convective transport into the upper troposphere, horizontal advection within the anticyclone at 200 hPa, distinct but measurable gradients at the westward edge of the vortex and formation of a secondary dynamical feature over the Asian Pacific. The data for C_2H_2 strongly support evidence for a strong isolated core to the anticyclone with distinct gradients surrounding this core. Within this region, there is a relatively lower correlation of C_2H_2 and CO suggesting difference in injection ratios or more likely due to expected chemical processing.

A second strong feature to the global distributions is observed in the enhancement and outflow of biomass burning from Africa at 200 hPa, both north-westward and eastward from 10° S. The easterly flow shows high C_2H_2 ratios to CO which have significantly decayed before reaching Australia. In the biomass burning regions, C_2H_2 and CO are relatively tightly correlated. C_2H_2 enhancements are observed to penetrate to

ACPD

10, 29735–29771, 2010

MIPAS retrievals Of acetylene

R. J. Parker et al.

Title Page

Abstract

Introduction

Conclusions

References

Tables

Figures

◀

▶

◀

▶

Back

Close

Full Screen / Esc

Printer-friendly Version

Interactive Discussion



lower altitudes in the African biomass outflow in this month compared to uplift observed in the Asian monsoon anticyclone region.

Overall, the data show the distinctive nature of C_2H_2 distributions, confirm in greater detail than previously possible features of hydrocarbon enhancements in the upper troposphere and highlight the future use of MIPAS hydrocarbon data for testing model transport and OH decay regimes in the middle to upper troposphere.

1 Introduction

The burning of vegetation, both living and dead, can release large quantities of gases into the atmosphere. Biomass burning is therefore a major source for the injection of trace gases into the atmosphere. Biomass burning and combustion were thought to be the major sources of acetylene (C_2H_2) (Hegg et al., 1990; Blake et al., 1996; Whitby and Altwicker, 1978). However, recent work also suggests that biofuel emissions may contribute as the dominant source of C_2H_2 with Xiao et al. (2007) estimating that as much as half of the global C_2H_2 source is due to biofuel (3.3 Tg yr^{-1}) with the remainder being due to fossil fuel (1.7 Tg yr^{-1}) and biomass burning (1.6 Tg yr^{-1}). Streets et al. (2003) found from their emission study that 45% of the C_2H_2 emissions in Asia were due to biofuel. It should be noted that Streets et al. (2003) make a clear distinction between what they term open biomass burning (i.e. forest fires) and the combustion of biofuels (wood, crop residue, dung, etc.) in domestic cooking and heating. The importance of biofuel as a C_2H_2 source has also been identified in Africa, where Bertschi et al. (2003) state that in their study of Zambia, the emission of C_2H_2 due to biofuel was significantly greater than that due to savanna biomass burning.

As it is estimated that Asia accounts for around 70% of global biofuel emissions as well as being a significant source for biomass burning and industrial emissions, it follows that Asia is the major source of C_2H_2 emissions. Africa is also an important source of C_2H_2 emissions, whether through biomass burning, fossil fuel or biofuel emissions. The work presented here is intended to confirm the large C_2H_2 concentrations emanating from these regions.

MIPAS retrievals Of acetylene

R. J. Parker et al.

Title Page

Abstract

Introduction

Conclusions

References

Tables

Figures

◀

▶

◀

▶

Back

Close

Full Screen / Esc

Printer-friendly Version

Interactive Discussion



MIPAS retrievals Of acetylene

R. J. Parker et al.

[Title Page](#)[Abstract](#)[Introduction](#)[Conclusions](#)[References](#)[Tables](#)[Figures](#)[◀](#)[▶](#)[◀](#)[▶](#)[Back](#)[Close](#)[Full Screen / Esc](#)[Printer-friendly Version](#)[Interactive Discussion](#)

It has been shown that the concentration of C_2H_2 is strongly correlated to CO and the ratio of the two can be used as a robust tracer for the photochemical evolution of the air mass since it last encountered a combustion source (Xiao et al., 2007) due to the relatively long life-times involved and the fact that the correlation remains strong over this period. This allows the relative photochemical age of biomass plumes to be estimated as well as the amount of photochemical processing that the plume has undergone.

In addition to the interest in C_2H_2 as a tracer for the transport of biomass/biofuel burning, C_2H_2 in itself plays an important role in the formation of glyoxal (CHOCHO) and has implications for the production of secondary organic aerosol (SOA) as discussed by Volkamer et al. (2009). For this reason, the ability to retrieve global distributions of C_2H_2 may also prove important for future air quality and climate simulations, hence this study.

Whilst vertical profiles of C_2H_2 have been observed from aircraft measurements (Smyth et al., 1996; Talbot et al., 2003) and more recently from satellite observations (Rinsland et al., 2005), there is still some uncertainty as to the distribution of C_2H_2 due to the poor understanding of the emissions from the large number of varying sources (Streets et al., 2003). Recent work by Park et al. (2008) has observed enhancements of C_2H_2 inside the Asian monsoon anticyclone from space with the Atmospheric Chemistry Experiment (ACE) FTIR instrument (Bernath et al., 2005). Due to the solar occultation technique used there are relatively few observations over the tropical region, with the majority of ACE observations occurring at polar latitudes. This sparse spatial sampling makes it necessary, particularly in the tropics, to average occultation data over multiple months and years.

In this paper, a description is provided of global retrievals of C_2H_2 performed from MIPAS infrared limb emission spectra for the upper troposphere. These provide greater temporal and spatial resolution than the ACE instrument albeit with a much lower signal to noise ratio (SNR) compared to the solar occultation method employed by ACE. Despite the higher noise, high spatial resolution distributions of C_2H_2 are successfully

determined on sub-monthly timescales. The results of this paper focus on the distribution for August 2003, a characteristic summer month where the influence of the Asian monsoon anticyclone is observed in conjunction with considerable fire activity in Africa.

2 The MIPAS instrument

5 The Michelson Interferometer for Passive Atmospheric Sounding (MIPAS) is a core instrument onboard the ENVironmental SATellite (ENVISAT) Satellite launched in March 2002. Measurements are performed by mid-infrared limb emission sounding of the atmosphere with a nominal mode (March 2002–March 2004) of 17 tangent altitudes at 68 km, 60 km, 52 km, 47 km, 42 km and then every 3 km until the final mid-tropospheric measurement at 6 km. MIPAS is a Fourier transform infrared spectrometer with a 10 0.025 unapodised spectral resolution and measures over a large spectral range, from 685 cm^{-1} to 2410 cm^{-1} , observing the region of the atmospheric spectrum where there are a variety of molecules with vibration-rotation bands with well-defined absorption lines (Fischer et al., 2008). Due to this, MIPAS is able to detect a wide range of trace species and is operationally used to retrieve pressure, temperature, O_3 , H_2O , CH_4 , HNO_3 , N_2O and NO_2 from 6 to 68 km (Raspollini et al., 2006). In addition, various non-operational trace species have been detected and retrieved from MIPAS spectra including PAN (Moore and Remedios, 2010; Glatthor et al., 2007), HCFC-22 (Moore and Remedios, 2008) and C_2H_6 (von Clarmann et al., 2007).

20 This work utilises the full resolution L1B MIPAS spectra from August 2003 where the instrument was measuring at 17 vertical levels with an unapodised spectral resolution of 0.025 cm^{-1} before technical issues resulted in a reduction in resolution to 0.06 cm^{-1} after August 2004.

MIPAS retrievals Of acetylene

R. J. Parker et al.

Title Page

Abstract

Introduction

Conclusions

References

Tables

Figures

◀

▶

◀

▶

Back

Close

Full Screen / Esc

Printer-friendly Version

Interactive Discussion



3 Determination of C₂H₂ in the upper troposphere

The objective of this work was to examine the C₂H₂ spectral signatures in MIPAS L1B spectra with a full optimal estimation retrieval algorithm in order to identify regions of high C₂H₂ volume mixing ratios (VMRs). These regions will be discussed in the context of their production and transport due to biomass burning.

The C₂H₂ infrared signature in the microwindow used for this work is outlined in Fig. 1 where the contributions from each species to the total radiance (black) are shown. The Oxford Reference Model (RFM) (Dudhia, 2005b) was used to model the spectra as observed by MIPAS. The RFM is a line-by-line radiative transfer model based on the GENLN2 model (Edwards, 1992) and can simulate the MIPAS infrared spectra taking into account the instrument lineshape and field of view. The spectroscopic information is taken from the HITRAN2004 spectral database (Rothman et al., 2005; Jacquemart et al., 2003) and in this case the simulation uses a standard atmospheric climatology (Remedios et al., 2007) with an enhancement of the C₂H₂ profile typical of biomass burning taken from Rinsland et al. (2005).

In Fig. 1, one line of the ν_5 band of C₂H₂ (purple line) can be seen to be the dominant feature in the 776.0 cm⁻¹ to 776.15 cm⁻¹ spectral range and unlike other C₂H₂ spectral lines in this region at 755 cm⁻¹, 762 cm⁻¹ and 766.7 cm⁻¹ the line is not masked by a strong ozone feature (Rinsland et al., 1998). This clear absorption line allows the unambiguous identification of enhanced C₂H₂ in MIPAS L1B spectra in this microwindow.

3.1 Retrieval method

A full optimal estimation approach was taken to retrieve the C₂H₂ VMR. The MIPAS Orbital Retrieval using Sequential Estimation or MORSE (Dudhia, 2005a) scheme is an optimal estimation scheme developed by the University Of Oxford based on the approach taken by Rodgers (2000) and has recently been used to successfully retrieve peroxyacetyl nitrate (PAN) from MIPAS observations by Moore and Remedios (2010) where further details of the retrieval scheme are provided.

MIPAS retrievals Of acetylene

R. J. Parker et al.

Title Page

Abstract

Introduction

Conclusions

References

Tables

Figures

◀

▶

◀

▶

Back

Close

Full Screen / Esc

Printer-friendly Version

Interactive Discussion



MIPAS retrievals Of acetylene

R. J. Parker et al.

Title Page

Abstract

Introduction

Conclusions

References

Tables

Figures

◀

▶

◀

▶

Back

Close

Full Screen / Esc

Printer-friendly Version

Interactive Discussion



The MORSE approach involves the inversion of the measured spectral radiances (\mathbf{y}) in order to obtain the best solution for the retrieved parameters (the state vector \mathbf{x}) with the associated random error, ϵ . The relationship between the retrieved parameters and the measured radiances is defined by a forward model $\mathbf{F}(\mathbf{x})$, in this case the RFM, which performs the radiative transfer calculations to calculate the expected radiance given the input parameters.

As described by Rodgers (2000), the solution to the above is constrained with respect to the a priori information (in this case standard climatologies) by the a priori covariance and the solution is found by minimising the cost function χ^2 via an iterative procedure where the state vector (\mathbf{x}) is updated after each iteration.

This iterative procedure for the state vector is

$$\mathbf{x}_{i+1} = \mathbf{x}_i - (\mathbf{S}_a^{-1} + \mathbf{K}_i^T \mathbf{S}_y^{-1} \mathbf{K}_i + \gamma \mathbf{D})^{-1} (-\mathbf{K}_i^T \mathbf{S}_y^{-1} [\mathbf{y} - \mathbf{F}(\mathbf{x}_i)] + \mathbf{S}_a^{-1} [\mathbf{x}_i - \mathbf{x}_a]) \quad (1)$$

with the cost function taking the form

$$\chi^2 = (\mathbf{y} - \mathbf{K}\mathbf{x})^T \mathbf{S}_y^{-1} (\mathbf{y} - \mathbf{K}\mathbf{x}) + (\mathbf{x} - \mathbf{x}_a)^T \mathbf{S}_a^{-1} (\mathbf{x} - \mathbf{x}_a) \quad (2)$$

\mathbf{S}_a is the a priori covariance matrix where diagonal values equivalent to a 1000% covariance of the C_2H_2 VMR along with a correlation length of 3 km were necessary to account for the large variations in VMR over biomass burning regions. \mathbf{S}_y is the measurement error covariance and was taken to be equivalent to a conservative estimate of the MIPAS spectral noise in Band A of $40 \text{ nW}/(\text{cm}^2 \text{ sr cm}^{-1})$ (Fischer et al., 2008); note that the noise in apodised spectra can reduce to lower than $20 \text{ nW}/(\text{cm}^2 \text{ sr cm}^{-1})$.

The reduction of the cost function at each iteration is used to test for convergence and the final value is useful in determining whether the obtained solution is a sensible value. Ideally, the value for χ^2 should be equal to the number of degrees of freedom in the retrieval.

In addition, in order to accurately retrieve C_2H_2 it was necessary to obtain accurate VMRs of the other interfering species in the spectral range. Therefore, prior to retrieving C_2H_2 , MORSE was used to retrieve profiles of pressure/temperature, H_2O , O_3 and

HNO₃ respectively which allowed an improvement to the climatology provided as a priori knowledge for subsequent retrievals.

3.2 Retrieval setup

C₂H₂ VMRs were retrieved for August 2003 for the 9 km to 30 km nominal MIPAS altitudes. The results presented in this paper are primarily for the upper-tropospheric limb measurements at a 12 km nominal altitude with a corresponding average pressure of 200 hpa. The retrieval used MORSE L1C files which were created by extracting the relevant radiance information for the C₂H₂ microwindow from the MIPAS L1B spectra and applying a Norton-Beer Medium apodisation. The retrieved data was filtered to remove points where the retrieval quality was not deemed to be satisfactory using the χ^2 parameter and a cloud index (Spang et al., 2004) value as indications of the quality of the retrieval. Only retrieved data where the cloud index was greater than 4.0 (corresponding to clear-sky conditions) and the χ^2 value was less than 2.0 were used. As a further indication of the retrieval quality, comparisons were performed to confirm that there were only small differences between the measured and simulated spectra in the retrieval process. These residuals are shown in Fig. 2 where average residuals of less than 40 nW/(cm² sr cm⁻¹) were found, consistent with MIPAS measurement noise. Encouragingly the mean bias in the residuals (dashed line in Fig. 2) is also small.

3.3 Error analysis

Figure 3 shows the final errors calculated for the retrieval, showing the total calculated error (solid line), along with the random component (dotted line) and the systematic component (dashed line). The systematic model parameter errors shown for each variable are 1 σ values calculated from measured biases in the MIPAS data and were taken from Fischer et al. (2008). Uncertainties of 2% were assumed for pressures and 1 K for temperatures. Water vapour was assumed to have an uncertainty of 20%, with 10% for O₃ and HNO₃ and 5% for CCl₄. The errors associated with the Gain, Shift

MIPAS retrievals Of acetylene

R. J. Parker et al.

Title Page

Abstract

Introduction

Conclusions

References

Tables

Figures

◀

▶

◀

▶

Back

Close

Full Screen / Esc

Printer-friendly Version

Interactive Discussion



and Spread were calculated using perturbations to the instrument line shape of 4%, 2% and 4% respectively and an offset error of $2 \text{ nW}/(\text{cm}^2 \text{ sr cm}^{-1})$ was assumed, with these figures taken from Fischer et al. (2008). The error relating to the C_2H_2 spectroscopy was conservatively assumed to be 5% with Jacquemart et al. (2003) giving an error of
5 between 2% and 5%.

The total error on the retrieved VMR was estimated to be 15.6% at 200 hpa, with the majority being related to the random retrieval noise (14%) and only 6.9% related to the systematic errors. Of those systematic errors, the uncertainty in the C_2H_2 spectroscopy and instrument line-shape effects along with the uncertainty in the pressure
10 and temperature were the dominant contributors; there is only a minimal contribution from the uncertainty in the VMRs of other species in this spectral window. As the C_2H_2 profile decreases rapidly with altitude, above 120 hpa there is a greatly reduced signal and hence the random error increases substantially. At these high altitudes the O_3 and HNO_3 uncertainties add to the overall error whilst at lower altitudes (300 hpa and
15 above), the uncertainty in water vapour VMR has a much larger affect.

4 C_2H_2 retrieval results

4.1 Global behaviour

Initially in the results that follow we concentrate on the 200 hpa level, at which the errors are smallest and random error dominates single profile retrievals.

Figure 4a shows all of the data at 200 hpa for the MORSE retrievals which pass the cloud and quality filters during August 2003. The data are averaged onto a regular grid with a 5° resolution using a distance-weighted approach to calculate the mean; a scaling distance r of 10° from the grid box centre is adopted with the weighting contribution following a $1 - x^2/r^2$ relationship, with the contribution reaching zero at
20 10° from the box centre (i.e. at $x = r$). This method maintained the sharper gradients reasonably well as well as producing a robust average of the individual observation
25

MIPAS retrievals Of acetylene

R. J. Parker et al.

[Title Page](#)[Abstract](#)[Introduction](#)[Conclusions](#)[References](#)[Tables](#)[Figures](#)[◀](#)[▶](#)[◀](#)[▶](#)[Back](#)[Close](#)[Full Screen / Esc](#)[Printer-friendly Version](#)[Interactive Discussion](#)

values. The data are not interpolated vertically to avoid interpolation errors and the average pressure of each set of retrieval levels is given instead, following the procedure of Moore and Remedios (2010).

The plot shows some key features of the C_2H_2 distributions observed in the August timeframe. Strong signals of source regions and transport of higher C_2H_2 mixing ratios are seen over the African biomass burning region and the Pacific outflow from Asia. In addition, a strong enhancement of C_2H_2 is observed over the Middle-Eastern region and clearly shows the enhanced C_2H_2 VMRs due to the Asian monsoon anticyclone as also reported by Park et al. (2008). Only a small signature is seen in the vicinity of the Amazon. It is also noticeable that the distributions in the most northerly latitudes, whilst greater than those in the corresponding southerly latitudes, are much lower in mixing ratio than in the extended African and Asian outflows.

4.2 C_2H_2 – CO relationships

The VMR of carbon monoxide is expected to be heavily correlated to that of C_2H_2 (Wang et al., 2004) with the ratio between the two acting as an indicator for the relative age of the air mass and the extent of atmospheric processing it has undergone (Xiao et al., 2007; Smyth et al., 1996, 1999). Hence in order to examine the C_2H_2 – CO relationship further the 150 hpa MOPITT (Measurement Of Pollution In The Troposphere) Level 2 Version 3 data for the same time period has also been investigated. Maps of the concentrations of the two gases are shown in Fig. 4.

The comparison of the two maps largely supports the interpretation that there is much in common between the two gases with respect to major inputs to the upper troposphere. However, there are also interesting differences. The C_2H_2 mixing ratios do not show strong features over Northern high latitudes and the Amazon unlike the CO data. In the Pacific region, the C_2H_2 appears to provide a tighter definition of the local transport, close to Asia, rather than the CO which appears more even in VMR, indicating that C_2H_2 distributions may prove useful in further constraining particular transport pathways. These aspects indicate that C_2H_2 data could provide some significant and complementary information to those contained in CO distributions.

MIPAS retrievals Of acetylene

R. J. Parker et al.

Title Page

Abstract

Introduction

Conclusions

References

Tables

Figures

◀

▶

◀

▶

Back

Close

Full Screen / Esc

Printer-friendly Version

Interactive Discussion



MIPAS retrievals Of acetylene

R. J. Parker et al.

[Title Page](#)[Abstract](#)[Introduction](#)[Conclusions](#)[References](#)[Tables](#)[Figures](#)[◀](#)[▶](#)[◀](#)[▶](#)[Back](#)[Close](#)[Full Screen / Esc](#)[Printer-friendly Version](#)[Interactive Discussion](#)

Some care should be taken in interpreting detailed comparisons of the two data sets as whilst MIPAS is observing at a 12 km nominal altitude with an approximate 3 km field of view and a mean pressure of 200 hpa, MOPITT is a nadir-sounding instrument with the retrieved vertical levels a result of its broad averaging kernels in the troposphere.

Typically the MOPITT CO 150 hpa averaging kernels have sensitivity between 400–100 hpa. We have estimated, by applying averaging kernels to typical profiles, that the effect of vertical resolution may lead to a systematic underestimation of the C₂H₂/CO ratio of approximately 10% but that a strong correlation would still be expected between the relevant trace gas data from these two instruments.

The strong African biomass burning signature is clearly observed in both datasets, indicating that a C₂H₂ enhancement due to biomass burning is present. In addition, there are strong CO and C₂H₂ enhancements observed over Asia, particularly the Asian outflow into the Northern Pacific Ocean. Although the data in the South-East Asia region is more sparse due to the cloud associated with the Asian monsoon, enhancements are observed over this region where data is present.

It is the strong enhancement of both CO and C₂H₂ in the Middle East region which is of particular interest. Rather than local production, the probable cause of this feature is long-range transport from the convective region over South-East Asia via the Easterly Jet associated with the Asian monsoon anticyclone into the Middle East.

It is expected that C₂H₂ is highly correlated to CO and the C₂H₂/CO ratio can provide important information relating to the age of the biomass plume and the amount of atmospheric processing it has undergone (Xiao et al., 2007). For this purpose, the 200 hpa MORSE C₂H₂ VMRs were correlated against the 150 hpa MOPITT CO VMRs for the globally averaged monthly data and the result is shown in Fig. 5a with the red points indicating the mean values of the data along with their standard deviation, separated into 2 ppbv bins. This figure clearly shows a strong correlation between the two VMRs (with $r = 0.76$) but at the same time, there appear to be two distinct domains within this correlation with distinctly different gradients.

MIPAS retrievals Of acetylene

R. J. Parker et al.

Title Page

Abstract

Introduction

Conclusions

References

Tables

Figures

◀

▶

◀

▶

Back

Close

Full Screen / Esc

Printer-friendly Version

Interactive Discussion



To examine this further, the correlation was performed separately for the Northern Hemisphere (Fig. 5b) and the Southern Hemisphere (Fig. 5c). From the C_2H_2 -CO correlations it becomes apparent that the two domains seen in the global correlation are due to the combination of the differences in C_2H_2 sources and transport between the two hemispheres. The strong correlation of 0.92 for the Southern Hemisphere is due to the lack of significant sources of C_2H_2 or long-range transport south of the equator whereas not only does the Northern Hemisphere contain the strong Asian C_2H_2 sources but there is a considerably higher background of CO in the Northern Hemisphere when compared to the Southern Hemisphere resulting in a lower correlation of 0.67. The tail of low C_2H_2 values compared to high CO values in the Northern Hemisphere plot stems from the high latitude data where CO is enhanced in a number of features whereas C_2H_2 is not.

The major biomass burning regions of Southern Africa (30° S to 10° N, 30° W to 80° E) and South America (30° S to 10° N, 180° W to 30° W) both show strong correlations, 0.81 (Fig. 6a) and 0.80 (Fig. 6b) respectively. However, the regions are otherwise very different. The highest C_2H_2 VMRs of 150 pptv are observed directly over the African source region, whereas the Amazon region shows much smaller C_2H_2 VMRS for the same CO mixing ratios. In the African sector, where significant transport into the Atlantic is observed, the gradient of the correlation is significantly higher (3.17) than in South America (1.41) indicating either very different source ratios of the two gases or else a very different photochemical regime. It is interesting to note that the South American gradient is the smallest of the four regions studied here.

For the region containing the eastward Asian outflow into the Pacific Ocean (10° N to 40° N, 130° E to 110° W), a correlation of 0.91 is observed (Fig. 6c) with a steep gradient (5.25). This strong correlation and steep gradient suggest that there is considerable transport between Asia and North America and that this occurs on a relatively short time-scale before the C_2H_2 has time to photochemically age.

Finally, the correlation for the Asian monsoon anticyclone region (10° N to 40° N, 30° E to 110° E) has a value of 0.59 (Fig. 6d). Unlike the previous examples, the region here is largely isolated with convective injection toward the east (see Sect. 4.4). Although the correlation is reasonable, it appears that there is considerable variability in either source ratios of C₂H₂ to CO or in the photochemical age of the C₂H₂ observed.

Having illustrated that the C₂H₂ and CO relationship maintains a largely strong correlation and remains preserved through the processes of convection and mixing as suggested by Smyth et al. (1996), the C₂H₂/CO ratio can be used to further analyse the transport dynamics from the combustion source regions and to explore further the transport out of the injection regions into the upper troposphere. The gridded C₂H₂ and CO values (as shown in Fig. 4) are used to calculate the C₂H₂/CO ratio (Fig. 7). The ratio is expected to be highest over source regions where C₂H₂ and CO are both produced from the combustion process and diminish with time as the photochemical age of air increases with atmospheric processing. Due to the difference in lifetimes of C₂H₂ (approximately 2 weeks) and CO (approximately 2 months), for a high C₂H₂/CO ratio to exist, the C₂H₂ must be relatively young. Hence, if a high C₂H₂/CO ratio is observed (i.e. greater than 2 pptv/ppbv, Smyth et al., 1996) then either the observation is over a region where combustion is taking place or the observed plume has been transported from such a source region in a relatively short space of time.

It is therefore possible to identify clear transport mechanisms from the C₂H₂/CO ratio in Fig. 7. The high ratio located over southern Africa is maintained as the plume travels north-west out into the Atlantic Ocean. In contrast, the eastward transport of this southern African plume towards the Indian Ocean and Australia would appear to be relatively slower, allowing the plume time to undergo a significant amount of atmospheric processing. A further transport pathway is observed from Asia out into the Pacific Ocean and is related to the tongue of the Asian Monsoon anticyclone that extends out over the Pacific. This process is known to transport air relatively quickly and this is confirmed by the fact that a high C₂H₂/CO ratio is maintained out over the ocean where there are no source regions present.

MIPAS retrievals Of acetylene

R. J. Parker et al.

Title Page

Abstract

Introduction

Conclusions

References

Tables

Figures

◀

▶

◀

▶

Back

Close

Full Screen / Esc

Printer-friendly Version

Interactive Discussion



MIPAS retrievals Of acetylene

R. J. Parker et al.

Title Page

Abstract

Introduction

Conclusions

References

Tables

Figures

◀

▶

◀

▶

Back

Close

Full Screen / Esc

Printer-friendly Version

Interactive Discussion



The fact that the C_2H_2/CO ratio agrees so closely with the known transport mechanisms in these regions provides substantial confidence in the approach taken. Furthermore, it allows the Easterly Jet transport from Asia into the Middle East to be discussed in the context of the C_2H_2/CO ratio. The high C_2H_2/CO ratio extends over the whole of the region between Asia and the Middle East and again clearly shows the strong chemical isolation of the monsoon. As this region is entirely over land some care must be taken to distinguish between a maintained high ratio due to fast transport or the alternative that the ratio remains high due to there being various combustion sources distributed over the whole region. There is no CO enhancement in the MOPITT surface data in this region and the correlation for this region (Fig. 6d) remains relatively strong. Along with this, the fact that a clear gradient exists in the distribution of the high C_2H_2 and CO values (Fig. 4) between the Middle East and Northern Africa provides confidence that it is the Easterly Jet transport that is being observed. The anticyclone continues to transport newly formed C_2H_2 and CO into the region from the biomass and biofuel sources in Asia, leaving no time for substantial photochemical processing to occur before it is circulated back towards the source region. It is this circulation due to the monsoon anticyclone which causes the persistence of the high C_2H_2/CO which is observed.

To summarise this section, the C_2H_2 -CO relationship has been examined for a variety of regions and it was found that strong correlations persist between the two species following transport into the upper troposphere. This in turn justified the use of a C_2H_2/CO ratio in order to examine characteristics of the observed transport pathways as well as identifying the chemical isolation due to the Asian monsoon anticyclone. The observation of ratios greater than 2 pptv/ppbv clearly suggests both localised injection and fast photochemical transport. In the following sections we examine in more detail the C_2H_2 distributions relating to African biomass burning and the Asian monsoon anticyclone.

4.3 African biomass burning

In order to examine some of the features of the C_2H_2 distributions in more detail, cross-sections have been plotted for both the meridional and zonal distributions. The NCEP mean tropopause pressure for August 2003 is shown as a red dashed line in order to give an indication of the location of the tropopause and to allow some preliminary discussion on whether any tropopause penetration into the stratosphere is being observed.

The C_2H_2 distribution relating to the African biomass burning is investigated through the use of zonal cross-sections taken along the $5^\circ N$ and $10^\circ S$ lines of latitude, passing through the African biomass burning C_2H_2 enhancement (Fig. 8). The cross-section taken along $5^\circ N$ shows how the large biomass burning signal is largely confined to below 250 hpa, well below the tropopause, with the outflow of C_2H_2 generally less than 100 pptv. The cross-section taken further south at $10^\circ S$ shows a similar distribution but this time with the strongest enhancement of C_2H_2 much more confined and extending somewhat higher into the atmosphere suggesting more intense biomass burning in this region associated with a greater uplift of C_2H_2 . Evidence for outflow of this biomass burning both towards the east and west is also apparent with C_2H_2 values above 100 pptv observed over both the Indian and Atlantic Oceans.

To examine this further, meridional cross-sections of the retrieved C_2H_2 distribution were taken along the $20^\circ E$ (Fig. 9a), $40^\circ E$ (Fig. 9b) and $75^\circ E$ (Fig. 9c) longitude lines.

The cross-section at $20^\circ E$ (Fig. 9a) passes through the western edge of the anticyclone in the Northern Hemisphere and through the large African biomass burning region in the Southern Hemisphere. The vertical transport of the C_2H_2 enhancement related to the African biomass burning is found to be relatively weak with the major enhancement ($C_2H_2 > 150$ pptv) only reaching 250 hpa. It is worth noting that in the stratospheric data, there are apparently weak enhancements of C_2H_2 above high values in the troposphere due to the African biomass region. Correlations suggests that these are a retrieval artefact and no other evidence of enhanced stratospheric values could be observed. This subject is returned to in the next section.

MIPAS retrievals Of acetylene

R. J. Parker et al.

Title Page

Abstract

Introduction

Conclusions

References

Tables

Figures

◀

▶

◀

▶

Back

Close

Full Screen / Esc

Printer-friendly Version

Interactive Discussion



This section has shown how the C_2H_2 retrieval from MIPAS is capable of providing information not only on the African biomass burning sources of C_2H_2 but also on the behaviour in terms of uplift and transport away from these sources.

4.4 The Asian monsoon anticyclone

In contrast to Africa, the strong C_2H_2 enhancement is observed as high as 150 hpa, reaching the tropopause in the meridional cross-section inside the core of the anticyclone at $75^\circ E$ (Fig. 9c). This suggests that the observed uplift from the monsoon convection is considerably stronger or occurs on a faster timescale compared to the weaker convection observed over Africa. The meridional distributions and outgoing longwave radiation (OLR) (Fig. 12b) show that the main monsoon convection is occurring between 0 and $20^\circ N$, with some convection extending further north. The data show very clearly that the C_2H_2 mixing ratios are very strongly related to the convective systems (see also Fig. 11). Following injection, the enhancement moves northwards and eastwards from the convective region into the centre of the anticyclone as the air is convected upwards. This also is consistent with the work of Park et al. (2007) who note a clear distinction between the location of the anticyclone circulation and the convective region over India and South-East Asia. The 150 hpa geopotential height anomaly calculated from NCEP meteorological data (Fig. 12a) shows the position of the Asian monsoon anti-cyclone and the associated wind field for this month.

Zonal cross-sections of C_2H_2 were taken along the $20^\circ N$ and $30^\circ N$ latitude lines passing through the strong Asian monsoon anticyclone isolation. The cross-section taken across the centre of the anticyclone core at $30^\circ N$ (Fig. 10a) shows the extent of the chemical isolation with a strong gradient of C_2H_2 both longitudinally between $20^\circ E$ and $50^\circ E$ at the western edge of the anticyclone and vertically as the C_2H_2 is constrained beneath the tropopause. The dramatic change in the C_2H_2 profiles across the monsoon boundary shows the strength of the chemical isolation inside the monsoon as previously identified by Park et al. (2008) but with much higher spatial and temporal resolution. It also clearly demonstrates the distinct gradient regions surrounding the

MIPAS retrievals Of acetylene

R. J. Parker et al.

Title Page

Abstract

Introduction

Conclusions

References

Tables

Figures

◀

▶

◀

▶

Back

Close

Full Screen / Esc

Printer-friendly Version

Interactive Discussion



monsoon anticyclone core. The zonal cross-section at 30° N (Fig. 10b) transects the convective region of the monsoon located over India and South-East Asia as indicated by OLR values less than 205 W/m² (Fig. 12b). Although the centre of the convective region contains no cloud-free data, the enhancements observed on the edge of this region support the suggestion that the C₂H₂ is uplifted from within this convective region. Finally, the zonal cross-section at 30° N (Fig. 10a) shows very nicely the eastward transport of enhanced VMRs at 200 hPa.

Figure 11 shows the C₂H₂ distributions at the four MIPAS levels with average pressures of 313, 200, 120 and 72 hPa (the 9, 12, 15 and 18 km nominal altitudes). Figure 11b at an average pressure of 200 hPa illustrates the convection-related uplift, the distinct gradients maintained around the core of the anti-cyclone and the enhancement of the VMRs in the core. In addition, one can observe a westward extension of the anticyclone which results in high mixing ratios in an apparent maximum near 160 degrees east. Such a feature could clearly be mis-interpreted in nadir sounding data emphasising the complementarity of good limb sounding observations.

In order to define the extent of the anticyclone system, the 150 hpa geopotential height anomaly is calculated from NCEP meteorological data (Fig. 12a) and confirms that the C₂H₂ is strongly isolated within the anticyclone core. The ability to capture the chemical isolation caused by the monsoon boundary so well in satellite data provides valuable information on the extent of its influence.

A set of typical averaging kernels for these C₂H₂ MIPAS retrievals over the monsoon anticyclone region are shown in Fig. 13 and clearly show strong peaks at approximately 300 hpa, 200 hpa and 120 hPa; for example, the 200 hpa averaging kernel peaks with a value of 0.72, indicating that there is a relatively small dependence on the a priori. The C₂H₂ response function above 120 hpa shows that these data are highly reflective of the 120 hPa level itself and so should be highly correlated with it. Our data reflect this in both global and local correlations (not shown). Therefore, although there is an interesting enhanced feature at 72 hPa in our data sets, we cannot assert that this feature is unambiguously a stratospheric enhancement since it overlies the enhanced

MIPAS retrievals Of acetylene

R. J. Parker et al.

Title Page

Abstract

Introduction

Conclusions

References

Tables

Figures

◀

▶

◀

▶

Back

Close

Full Screen / Esc

Printer-friendly Version

Interactive Discussion



VMRs in the troposphere below it. These vertical correlations in our retrievals suggest that interpretation of this feature in our MIPAS data set requires considerable care.

In a recent paper, Randel et al. (2010) identify the transport of air masses from the surface deep into the stratosphere through the use of HCN retrieved from ACE. They conclude that the monsoon circulation provides an effective pathway for pollution from Asia, India and Indonesia to enter the global stratosphere. It is not clear whether our retrievals are entirely sensitive to the stratosphere but they do show good promise for verifying model transport pathways in a given year.

This section has focused on the chemical isolation of the C_2H_2 distribution relating to the Asian monsoon anticyclone. The vertical and horizontal extent of this isolation has been mapped to a much higher spatial resolution than has previously been possible. The data compares well against other indicators of the location of the anticyclone such as the geopotential height, and shows both the strong eastward transport in the core of the vortex and the strong gradients at the edge of the vortex. The convective impact on C_2H_2 is very clear from our data using both the regions of cloudiness and the OLR. Enhancements of the VMR could not clearly be distinguished in the stratosphere due to vertical correlations in the retrievals.

5 Conclusions

C_2H_2 has been successfully retrieved from MIPAS for August 2003 with strong signatures associated with the Asian monsoon anticyclone chemical isolation and African biomass burning clearly evident.

Once retrieved, the C_2H_2 VMR has been used in conjunction with the 150 hpa MO-PITT CO VMR to examine the correlation between C_2H_2 and CO. When performed globally, these calculations showed a strong correlation between the C_2H_2 and CO of 0.76 but with two distinct domains due to the Northern and Southern Hemispheres. When correlated individual, the Northern Hemisphere had a correlation of 0.67 showing the much greater variability in the transport and sources compared to the Southern

MIPAS retrievals Of acetylene

R. J. Parker et al.

Title Page

Abstract

Introduction

Conclusions

References

Tables

Figures

◀

▶

◀

▶

Back

Close

Full Screen / Esc

Printer-friendly Version

Interactive Discussion



Discussion Paper | Discussion Paper | Discussion Paper | Discussion Paper | Discussion Paper

MIPAS retrievals Of acetylene

R. J. Parker et al.

[Title Page](#)[Abstract](#)[Introduction](#)[Conclusions](#)[References](#)[Tables](#)[Figures](#)[◀](#)[▶](#)[◀](#)[▶](#)[Back](#)[Close](#)[Full Screen / Esc](#)[Printer-friendly Version](#)[Interactive Discussion](#)

Hemisphere whose correlation was 0.918 but with significantly lower C_2H_2 values. Defining the geographical regions to limit the influence of the variability from different sources allowed stronger correlations to be revealed. Africa, South America, the Asian monsoon anticyclone and the Asian Pacific outflow regions all correlated strongly with the difference in gradients giving some indication of the amount of transport occurring in the different regions. Even for the case over the Middle East/Asia where there is no clear ocean background influence to distinguish the enhancements from, a reasonable correlation between C_2H_2 and CO still existed.

As the C_2H_2 and CO remain well correlated through transport and mixing, this allowed the C_2H_2/CO ratio to be calculated and analysed in the context of the photochemical age of air and the time since the air mass had last encountered a combustion source. From this analysis it was found that known transport mechanisms from Southern Africa into the Atlantic/Indian Oceans and the transport from Asia into the Pacific Ocean were well-defined with the relative speed of each transport system indicated by the C_2H_2/CO ratio. It was also noted that the C_2H_2 appeared to be more tightly confined along the transport pathways compared to the CO which due to its longer lifetime does become slightly more mixed. Furthermore, a strong C_2H_2 signal was retrieved over the Middle East region and the C_2H_2/CO ratio allowed us to observe enhanced C_2H_2 concentrations resulting from the fast outflow from Asia associated with the monsoon anticyclone. This enhancement was maintained by the influence of the anticyclone associated with the monsoon, which acts as a barrier to further transport and leads to the chemical isolation in the region. This was verified further through the use of trajectory modelling (not shown) which provided further confidence in both the C_2H_2 retrieval and in the use of the C_2H_2/CO ratio to act as an indicator for the photochemical age of air in future work.

By examining cross-sections through the anticyclone, the horizontal and vertical extent of the isolation was shown. The location of the convective region over India and South-East Asia as identified by OLR data was also evident from these cross-sections, suggesting that it is from this region where the C_2H_2 is convected into the

upper troposphere. Analysis of the geopotential height anomaly and 150 hpa wind vectors were also used to verify the location of the anticyclone which was found to be in very good agreement with the C_2H_2 distribution, identifying C_2H_2 as an appropriate dynamical tracer.

5 A similar analysis was performed for the African biomass burning enhancements. This showed the behaviour of the uplift, which was observed not to penetrate as high into the troposphere as for the Asian monsoon anticyclone. This, along with the observed outflow from this region, has allowed the areas of more intense biomass burning activity to be identified.

10 In summary, we have shown that it is possible to use MIPAS data to explore the upper-tropospheric distributions of C_2H_2 with a much higher temporal and spatial resolution than has previously been possible. The ratio of C_2H_2 -CO was shown to provide information on the transport of photochemically aged plumes and the amount of atmospheric processing they have undergone. In addition, we have shown that C_2H_2 can
15 act as a tracer not only for investigating effects such as transport and convection but also for identifying dynamical effects such as the monsoon's chemical isolation. Due to the high spatial sampling, this data would prove suitable for further exploitation by comparisons to modelled data in order to study these effects further.

20 *Acknowledgements.* Robert Parker was supported by a research studentship from the Natural Environment Research Council. David Moore was supported by the National Centre For Earth Observation (NCEO). Vijay Kanawade was supported from SPARTAN project contract number MEST-CT-2004-7512. The authors wish to thank the European Space Agency for access to MIPAS data under CUTLSOM (AO-357). The MOPITT Level 2 (L2) Version 3 data used in this study was obtained from the NASA Langley Research Center Atmospheric Science Data
25 Center. We would also like to thank Anu Dudhia for providing us with the Oxford Reference Forward Model (RFM) and the MIPAS Orbital Retrieval using Sequential Estimation (MORSE) code used in this study. The authors also gratefully acknowledge the NOAA Air Resources Laboratory (ARL) for the provision of the HYSPLIT transport and dispersion model used in this publication.

MIPAS retrievals Of acetylene

R. J. Parker et al.

Title Page

Abstract

Introduction

Conclusions

References

Tables

Figures

◀

▶

◀

▶

Back

Close

Full Screen / Esc

Printer-friendly Version

Interactive Discussion



References

- Bernath, P. F., McElroy, C. T., Abrams, M. C., Boone, C. D., Butler, M., Camy-Peyret, C., Carleer, M., Clerbaux, C., Coheur, P., Colin, R., DeCola, P., DeMazire, M., Drummond, J. R., Dufour, D., Evans, W. F. J., Fast, H., Fussen, D., Gilbert, K., Jennings, D. E., Llewellyn, E. J., Lowe, R. P., Mahieu, E., McConnell, J. C., McHugh, M., McLeod, S. D., Michaud, R., Midwinter, C., Nassar, R., Nichitiu, F., Nowlan, C., Rinsland, C. P., Rochon, Y. J., Rowlands, N., Semeniuk, K., Simon, P., Skelton, R., Sloan, J. J., Soucy, M., Strong, K., Tremblay, P., Turnbull, D., Walker, K. A., Walkty, I., Wardle, D. A., Wehrle, V., Zander, R., and Zou, J.: Atmospheric chemistry experiment (ACE): Mission overview, *Geophys. Res. Lett.*, 32, L15S01, doi:10.1029/2005GL022386, 2005. 29738
- Bertschi, I. T., Yokelson, R. J., Ward, D. E., Christian, T. J., and Hao, W. M.: Trace gas emissions from the production and use of domestic biofuels in Zambia measured by open-path Fourier transform infrared spectroscopy, *J. Geophys. Res. D: Atmos.*, 108, 8469, doi:10.1029/2002JD002158, 2003. 29737
- Blake, N. J., Blake, D. R., Sive, B. C., Chen, T. Y., Rowland, F. S., Collins Jr, J. E., Sachse, G. W., and Anderson, B. E.: Biomass burning emissions and vertical distribution of atmospheric methyl halides and other reduced carbon gases in the South Atlantic region, *J. Geophys. Res. Atmos.*, 101, 24151–24164, 1996. 29737
- Dudhia, A.: MIPAS Orbital Retrieval using Sequential Estimation, available at: <http://www.atm.ox.ac.uk/MORSE/>, 2005a. 29740
- Dudhia, A.: The Oxford Reference Forward Model, available at: <http://www.atm.ox.ac.uk/RFM/>, 2005b. 29740
- Edwards, D. P.: GENLN2: A general line-by-line atmospheric transmittance and radiance model. Version 3.0: Description and users guide, Report NCAR /TN-367 +STR, National Center for Atmospheric Research, Boulder, Col., 1992. 29740
- Fischer, H., Birk, M., Blom, C., Carli, B., Carlotti, M., von Clarmann, T., Delbouille, L., Dudhia, A., Ehhalt, D., Endemann, M., Flaud, J. M., Gessner, R., Kleinert, A., Koopman, R., Langen, J., López-Puertas, M., Mosner, P., Nett, H., Oelhaf, H., Perron, G., Remedios, J., Ridolfi, M., Stiller, G., and Zander, R.: MIPAS: an instrument for atmospheric and climate research, *Atmos. Chem. Phys.*, 8, 2151–2188, doi:10.5194/acp-8-2151-2008, 2008. 29739, 29741, 29742, 29743
- Glatthor, N., von Clarmann, T., Fischer, H., Funke, B., Grabowski, U., Höpfner, M., Kellmann,

MIPAS retrievals Of acetylene

R. J. Parker et al.

Title Page

Abstract

Introduction

Conclusions

References

Tables

Figures

◀

▶

◀

▶

Back

Close

Full Screen / Esc

Printer-friendly Version

Interactive Discussion



MIPAS retrievals Of acetylene

R. J. Parker et al.

Title Page

Abstract

Introduction

Conclusions

References

Tables

Figures

◀

▶

◀

▶

Back

Close

Full Screen / Esc

Printer-friendly Version

Interactive Discussion



S., Kiefer, M., Linden, A., Milz, M., Steck, T., and Stiller, G. P.: Global peroxyacetyl nitrate (PAN) retrieval in the upper troposphere from limb emission spectra of the Michelson Interferometer for Passive Atmospheric Sounding (MIPAS), *Atmos. Chem. Phys.*, 7, 2775–2787, doi:10.5194/acp-7-2775-2007, 2007. 29739

5 Hegg, D. A., Radke, L. F., Hobbs, P. V., Rasmussen, R. A., and Riggan, P. J.: Emissions of some trace gases from biomass fires, *J. Geophys. Res.*, 95, 5669–5675, 1990. 29737

Jacquemart, D., Mandin, J. Y., Dana, V., Claveau, C., Vander Auwera, J., Herman, M., Rothman, L., Regalia-Jarlot, L., and Barbe, A.: The IR acetylene spectrum in HITRAN: update and new results, *J. Quant. Spectrosc. Ra.*, 82, 363–382, 2003. 29740, 29743

10 Moore, D. P. and Remedios, J. J.: Growth rates of stratospheric HCFC-22, *Atmos. Chem. Phys.*, 8, 73–82, doi:10.5194/acp-8-73-2008, 2008. 29739

Moore, D. P. and Remedios, J. J.: Seasonality of Peroxyacetyl nitrate (PAN) in the upper troposphere and lower stratosphere using the MIPAS-E instrument, *Atmos. Chem. Phys.*, 10, 6117–6128, doi:10.5194/acp-10-6117-2010, 2010. 29739, 29740, 29744

15 Park, M., Randel, W. J., Gettelman, A., Massie, S. T., and Jiang, J. H.: Transport above the Asian summer monsoon anticyclone inferred from Aura Microwave Limb Sounder tracers, *J. Geophys. Res. Atmos.*, 112, D16309, doi:10.1029/2006JD008294, 2007. 29750

Park, M., Randel, W. J., Emmons, L. K., Bernath, P. F., Walker, K. A., and Boone, C. D.: Chemical isolation in the Asian monsoon anticyclone observed in Atmospheric Chemistry Experiment (ACE-FTS) data, *Atmos. Chem. Phys.*, 8, 757–764, doi:10.5194/acp-8-757-2008, 2008. 29738, 29744, 29750

20 Randel, W. J., Park, M., Emmons, L., Kinnison, D., Bernath, P., Walker, K. A., Boone, C., and Pumphrey, H.: Asian monsoon transport of pollution to the stratosphere, *Science*, 328, 611–613, 2010. 29752

25 Raspollini, P., Belotti, C., Burgess, A., Carli, B., Carlotti, M., Ceccherini, S., Dinelli, B. M., Dudhia, A., Flaud, J.-M., Funke, B., Höpfner, M., López-Puertas, M., Payne, V., Piccolo, C., Remedios, J. J., Ridolfi, M., and Spang, R.: MIPAS level 2 operational analysis, *Atmos. Chem. Phys.*, 6, 5605–5630, doi:10.5194/acp-6-5605-2006, 2006. 29739

30 Remedios, J. J., Allen, G., Waterfall, A. M., Oelhaf, H., Kleinert, A., and Moore, D. P.: Detection of organic compound signatures in infra-red, limb emission spectra observed by the MIPAS-B2 balloon instrument, *Atmos. Chem. Phys.*, 7, 1599–1613, doi:10.5194/acp-7-1599-2007, 2007. 29740

Rinsland, C. P., Gunson, M. R., Wang, P. H., Arduini, R. F., Baum, B. A., Minnis, P., Goldman,

MIPAS retrievals Of acetylene

R. J. Parker et al.

Title Page

Abstract

Introduction

Conclusions

References

Tables

Figures

◀

▶

◀

▶

Back

Close

Full Screen / Esc

Printer-friendly Version

Interactive Discussion



A., Abrams, M. C., Zander, R., Mahieu, E., Salawitch, R. J., Michelsen, H. A., Irion, F. W., and Newchurch, M. J.: ATMOS/ATLAS 3 infrared profile measurements of trace gases in the November 1994 tropical and subtropical upper troposphere, *J. Quant. Spectrosc. Ra.*, 60, 891–901, 1998. 29740

5 Rinsland, C. P., Dufour, G., Boone, C. D., Bernath, P. F., and Chiou, L.: Atmospheric Chemistry Experiment (ACE) measurements of elevated Southern Hemisphere upper tropospheric CO, C₂H₆, HCN, and C₂H₂ mixing ratios from biomass burning emissions and long-range transport, *Geophys. Res. Lett.*, 32, 1–4, 2005. 29738, 29740

Rodgers, C.: Inverse methods for atmospheric sounding: theory and practice, World Scientific, 2000. 29740, 29741

10 Rothman, L. S., Jacquemart, D., Barbe, A., Benner, D. C., Birk, M., Brown, L. R., Carleer, M. R., Chackerian Jr., C., Chance, K., Coudert, L. H., Dana, V., Devi, V. M., Flaud, J. ., Gamache, R. R., Goldman, A., Hartmann, J. ., Jucks, K. W., Maki, A. G., Mandin, J. ., Massie, S. T., Orphal, J., Perrin, A., Rinsland, C. P., Smith, M. A. H., Tennyson, J., Tolchenov, R. N., Toth, R. A., Vander Auwera, J., Varanasi, P., and Wagner, G.: The HITRAN 2004 molecular spectroscopic database, *J. Quant. Spectrosc. Ra.*, 96, 139–204, 2005. 29740

15 Smyth, S. B., Sandholm, S. T., Bradshaw, J. D., Talbot, R. W., Blake, D. R., Blake, N. J., Rowland, F. S., Singh, H. B., Gregory, G. L., Anderson, B. E., Sachse, G. W., Collins, J. E., and Bachmeier, A. S.: Factors influencing the upper free tropospheric distribution of reactive nitrogen over the South Atlantic during the TRACE A experiment, *J. Geophys. Res. Atmos.*, 101, 24165–24186, 1996. 29738, 29744, 29747

20 Smyth, S., Sandholm, S., Shumaker, B., Mitch, W., Kanvinde, A., Bradshaw, J., Liu, S., McKeen, S., Gregory, G., Anderson, B., Talbot, R., Blake, D., Rowland, S., Browell, E., Fenn, M., Merrill, J., Bachmeier, S., Sachse, G., and Collins, J.: Characterization of the chemical signatures of air masses observed during the PEM experiments over the western Pacific, *J. Geophys. Res. Atmos.*, 104, 16243–16254, 1999. 29744

25 Spang, R., Remedios, J. J., and Barkley, M. P.: Colour indices for the detection and differentiation of cloud types in infra-red limb emission spectra, *Adv. Space Res.*, 33, 1041–1047, 2004. 29742

30 Streets, D. G., Bond, T. C., Carmichael, G. R., Fernandes, S. D., Fu, Q., He, D., Klimont, Z., Nelson, S. M., Tsai, N. Y., Wang, M. Q., Woo, J. H., and Yarber, K. F.: An inventory of gaseous and primary aerosol emissions in Asia in the year 2000, *J. Geophys. Res. Atmos.*, 108, 8809, doi:10.1029/2002JD003093, 2003. 29737, 29738

MIPAS retrievals Of acetylene

R. J. Parker et al.

Title Page

Abstract

Introduction

Conclusions

References

Tables

Figures

I◀

▶I

◀

▶

Back

Close

Full Screen / Esc

Printer-friendly Version

Interactive Discussion



Talbot, R., Dibb, J., Scheuer, E., Seid, G., Russo, R., Sandholm, S., Tan, D., Singh, H., Blake, D., Blake, N., Atlas, E., Sachse, G., Jordan, C., and Avery, M.: Reactive nitrogen in Asian continental outflow over the western Pacific: Results from the NASA Transport and Chemical Evolution over the Pacific (TRACE-P) airborne mission, *J. Geophys. Res. Atmos.*, 108, 8803, doi:10.1029/2002JD003129, 2003. 29738

Volkamer, R., Ziemann, P. J., and Molina, M. J.: Secondary Organic Aerosol Formation from Acetylene (C_2H_2): seed effect on SOA yields due to organic photochemistry in the aerosol aqueous phase, *Atmos. Chem. Phys.*, 9, 1907–1928, doi:10.5194/acp-9-1907-2009, 2009. 29738

von Clarmann, T., Glatthor, N., Koukouli, M. E., Stiller, G. P., Funke, B., Grabowski, U., Höpfner, M., Kellmann, S., Linden, A., Milz, M., Steck, T., and Fischer, H.: MIPAS measurements of upper tropospheric C_2H_6 and O_3 during the southern hemispheric biomass burning season in 2003, *Atmos. Chem. Phys.*, 7, 5861–5872, doi:10.5194/acp-7-5861-2007, 2007. 29739

Wang, T., Wong, C. H., Cheung, T. F., Blake, D. R., Arimoto, R., Baumann, K., Tang, J., Ding, G. A., Yu, X. M., Li, Y. S., Streets, D. G., and Simpson, I. J.: Relationships of trace gases and aerosols and the emission characteristics at Lin'an, a rural site in eastern China, during spring 2001, *J. Geophys. Res. Atmos.*, 109, D19S05, doi:10.1029/2003JD004119, 2004. 29744

Whitby, R. A. and Altwicker, E. R.: Acetylene in the atmosphere: sources, representative ambient concentrations and ratios to other hydrocarbons, *Atmos. Environ.*, 12, 1289–1296, 1978. 29737

Xiao, Y., Jacob, D. J., and Turquety, S.: Atmospheric acetylene and its relationship with CO as an indicator of air mass age, *J. Geophys. Res. Atmos.*, 112, D12305, doi:10.1029/2006JD008268, 2007. 29738, 29744, 29745

MIPAS retrievals Of acetylene

R. J. Parker et al.

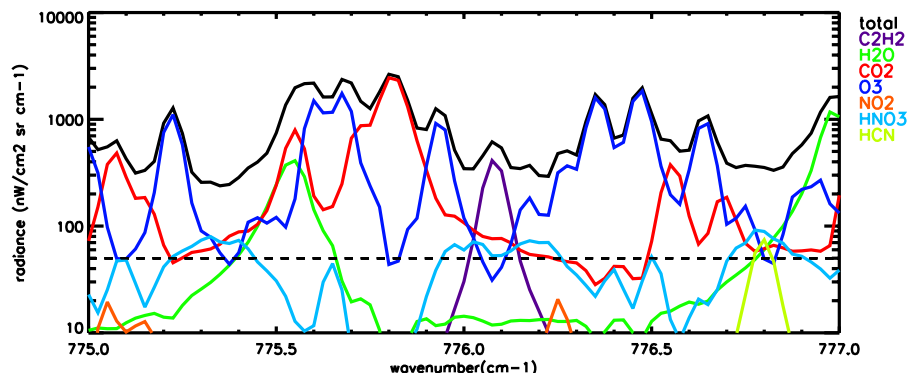


Fig. 1. RFM simulation of a 12 km MIPAS spectra at a 0.025 cm^{-1} resolution covering a 2 cm^{-1} range around the prominent C_2H_2 feature at 776.075 cm^{-1} . This shows the contribution to the C_2H_2 microwindow (776.0 cm^{-1} to 776.15 cm^{-1}) from interfering species and uses a standard atmosphere background with an enhanced C_2H_2 profile typical of biomass burning observations.

[Title Page](#)[Abstract](#)[Introduction](#)[Conclusions](#)[References](#)[Tables](#)[Figures](#)[◀](#)[▶](#)[◀](#)[▶](#)[Back](#)[Close](#)[Full Screen / Esc](#)[Printer-friendly Version](#)[Interactive Discussion](#)

MIPAS retrievals Of acetylene

R. J. Parker et al.

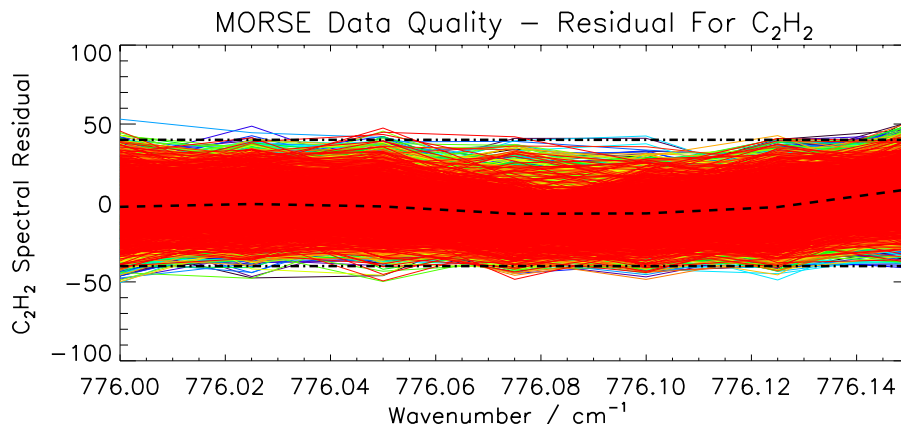


Fig. 2. All residuals for the C₂H₂ retrieval at the 12 km nominal altitude. The different coloured lines indicate each individual retrieval. The dashed line shows the mean value of all of the residuals and the dash-dot line shows the $\pm 40 \text{ nW}/(\text{cm}^2 \text{ sr cm}^{-1})$ values indicating the MIPAS measurement noise within which all of the retrieval residuals lie.

[Title Page](#)[Abstract](#)[Introduction](#)[Conclusions](#)[References](#)[Tables](#)[Figures](#)[◀](#)[▶](#)[◀](#)[▶](#)[Back](#)[Close](#)[Full Screen / Esc](#)[Printer-friendly Version](#)[Interactive Discussion](#)

MIPAS retrievals Of acetylene

R. J. Parker et al.

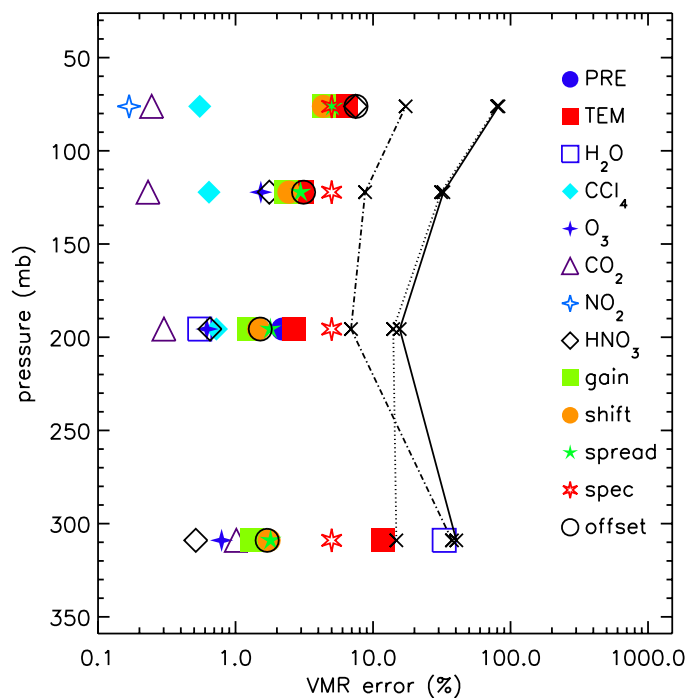


Fig. 3. Contributions to the C₂H₂ retrieval error. The total error (solid line), random error (dotted line) and the systematic error (dashed line) are all shown as well as the various components to the systematic error such as the Instrument Line Shape and spectroscopic errors.

Title Page

Abstract

Introduction

Conclusions

References

Tables

Figures

◀

▶

◀

▶

Back

Close

Full Screen / Esc

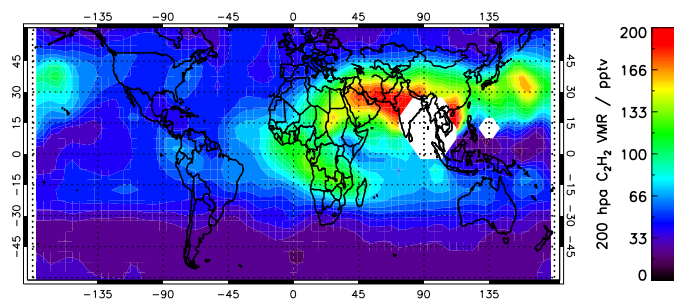
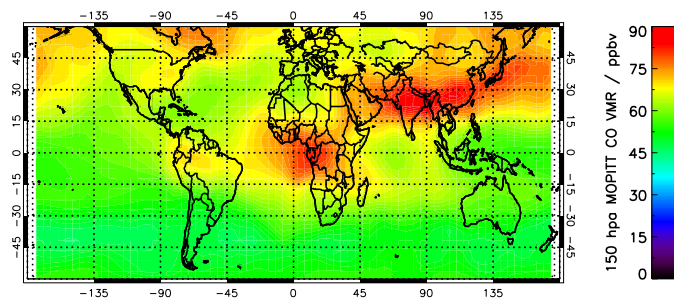
Printer-friendly Version

Interactive Discussion



MIPAS retrievals Of
acetylene

R. J. Parker et al.

(a) 200 hpa C_2H_2 

(b) 150 hpa MOPITT CO

Fig. 4. 200 hpa MORSE C_2H_2 VMRs and 150 hpa MOPITT CO VMRs averaged for August 2003. The strong chemical isolation related to the Asian monsoon anticyclone is the dominant feature but strong enhancements of both species are also observed relating to biomass burning in southern Africa and Asian outflow into the Pacific.

[Title Page](#)[Abstract](#)[Introduction](#)[Conclusions](#)[References](#)[Tables](#)[Figures](#)[◀](#)[▶](#)[◀](#)[▶](#)[Back](#)[Close](#)[Full Screen / Esc](#)[Printer-friendly Version](#)[Interactive Discussion](#)

MIPAS retrievals Of acetylene

R. J. Parker et al.

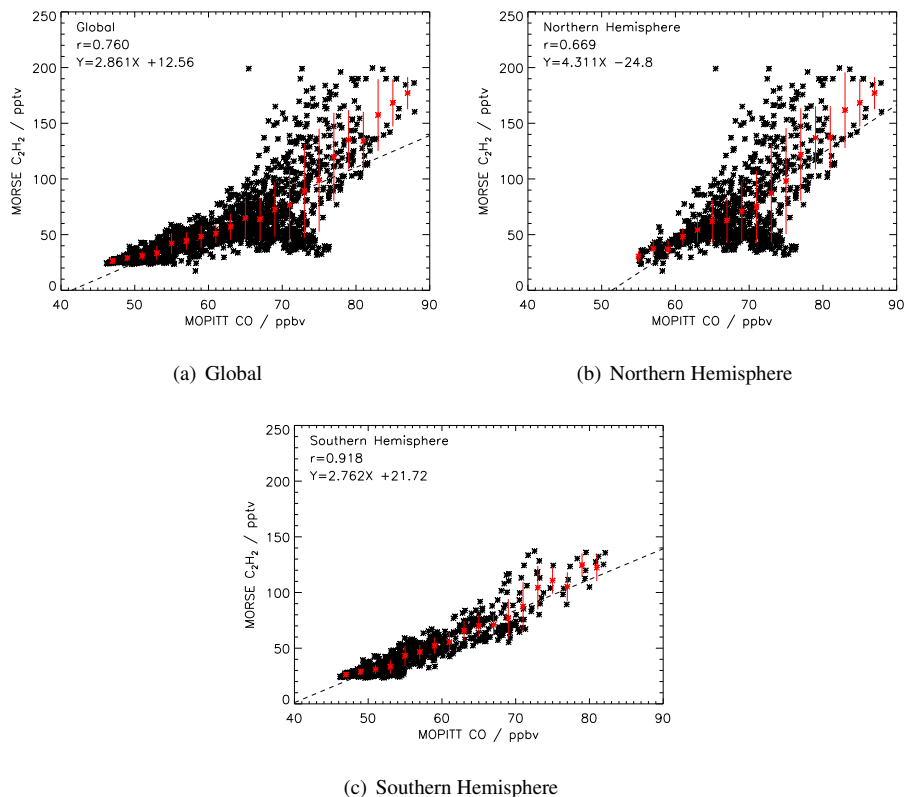


Fig. 5. Correlation of the 200 hpa MORSE C_2H_2 VMRs against 150 hpa MOPITT CO VMRs averaged for August 2003 for Globally, the Northern Hemisphere and the Southern Hemisphere. The two distinct domains observed in the global correlation are due to the differences in sources and transport for the Northern Hemisphere and Southern Hemisphere. The dashed lines indicate the line of best fit through the correlations. The red points show the average values in 2 ppbv bins, with the associated error bars indicating the standard deviation within each bin.

Title Page

Abstract

Introduction

Conclusions

References

Tables

Figures

◀

▶

◀

▶

Back

Close

Full Screen / Esc

Printer-friendly Version

Interactive Discussion



MIPAS retrievals Of acetylene

R. J. Parker et al.

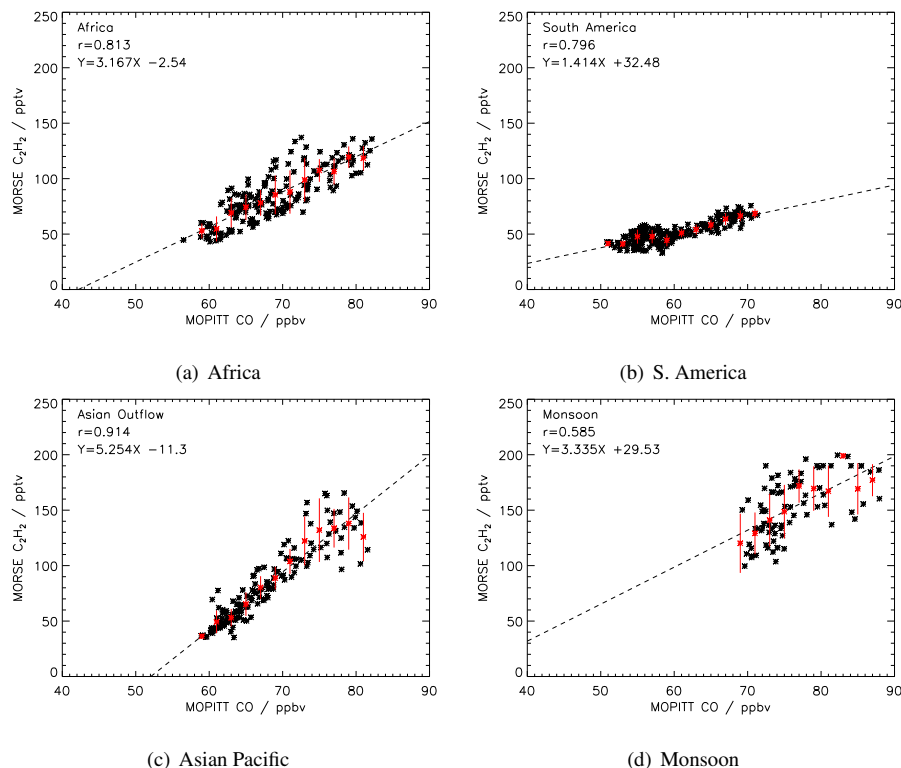


Fig. 6. 200 hpa MORSE C_2H_2 VMRs against 150 hpa MOPITT CO VMRs averaged for August 2003 for: Africa [30° S to 10° N, 30° W to 80° E], South America [30° S to 10° N, 180° W to 30° W], Asian Pacific Outflow [10° N to 40° N, 130° E to 110° W] and the Asian monsoon anticyclone region [10° N to 40° N, 30° E to 110° E]. Again, the dashed lines indicate the line of best fit through the correlations. The red points show the average values in 2 ppbv bins, with the associated error bars indicating the standard deviation within each bin.

Title Page

Abstract

Introduction

Conclusions

References

Tables

Figures

◀

▶

◀

▶

Back

Close

Full Screen / Esc

Printer-friendly Version

Interactive Discussion



MIPAS retrievals Of acetylene

R. J. Parker et al.

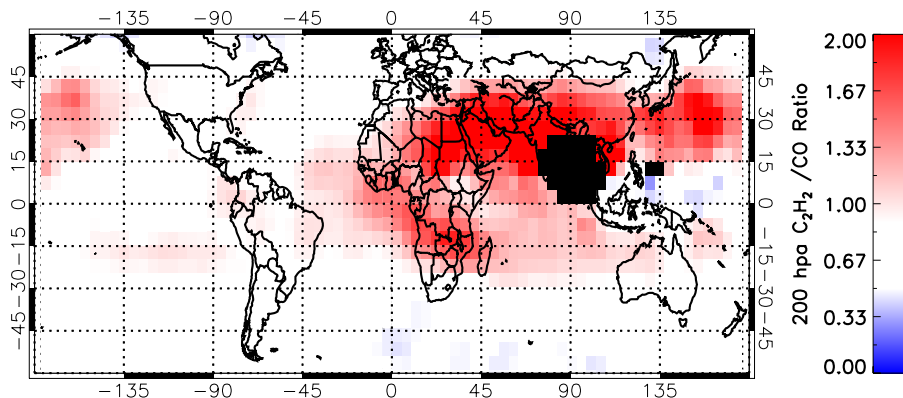
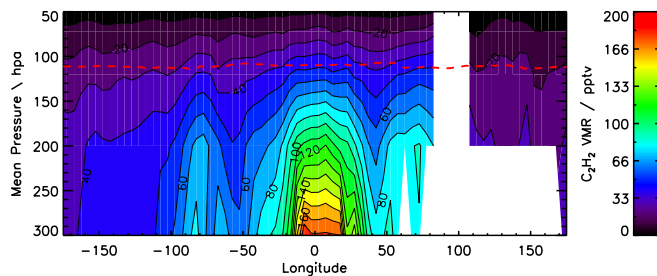


Fig. 7. 200 hpa MORSE C₂H₂/150 hpa MOPITT CO ratio calculated from the 5° N globally gridded data (in units of pptv/ppbv). This ratio acts as an indicator of biomass burning sources and age of air and hence provides information on the relative speed of transport mechanisms. Features of note include the transport from African biomass into the Atlantic, transport from Asia into the Pacific and the isolation of the monsoon anticyclone.

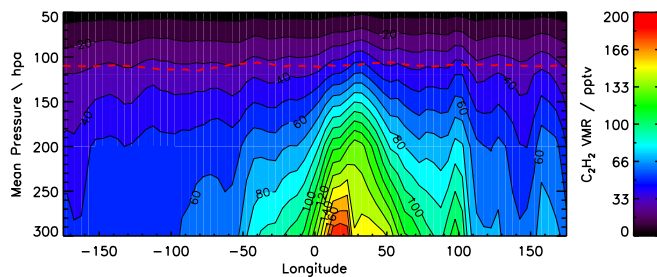
[Title Page](#)[Abstract](#)[Introduction](#)[Conclusions](#)[References](#)[Tables](#)[Figures](#)[◀](#)[▶](#)[◀](#)[▶](#)[Back](#)[Close](#)[Full Screen / Esc](#)[Printer-friendly Version](#)[Interactive Discussion](#)

MIPAS retrievals Of
acetylene

R. J. Parker et al.



(a) East-West along 5° N



(b) East-West along 10° S

Fig. 8. Zonal cross-sections of the retrieved C_2H_2 distributions along the 5° N and 10° S lines of latitude, passing through the African biomass burning C_2H_2 enhancement. The NCEP mean tropopause pressure for August 2003 is shown by the red dashed line.

Title Page

Abstract

Introduction

Conclusions

References

Tables

Figures

◀

▶

◀

▶

Back

Close

Full Screen / Esc

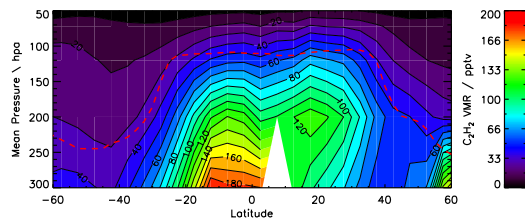
Printer-friendly Version

Interactive Discussion

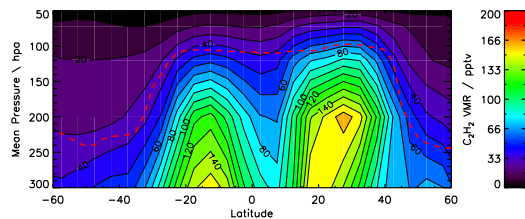


MIPAS retrievals Of acetylene

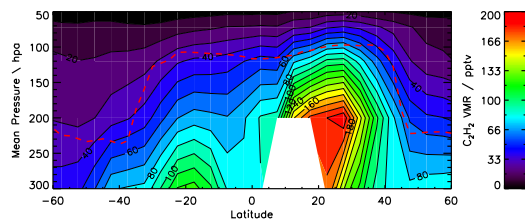
R. J. Parker et al.



(a) North-South along 20° E



(b) North-South along 40° E



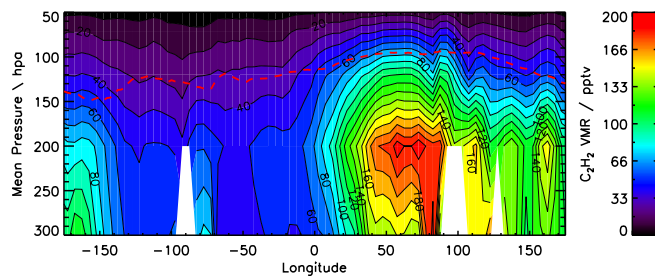
(c) North-South along 75° E

Fig. 9. Meridional cross-sections of the retrieved C₂H₂ distributions passing North-South through both the strong Asian monsoon anticyclone isolation and the African biomass burning enhancement at 20° E, 40° E and 75° E. The NCEP mean tropopause pressure for August 2003 is shown by the red dashed line.

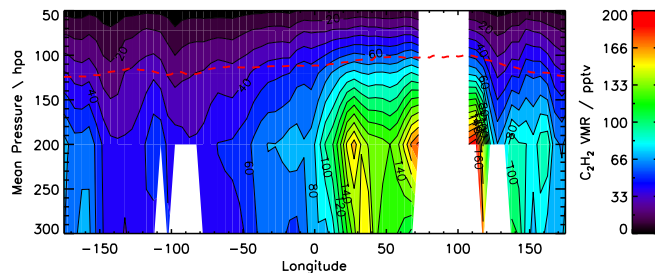
[Title Page](#)[Abstract](#)[Introduction](#)[Conclusions](#)[References](#)[Tables](#)[Figures](#)[◀](#)[▶](#)[◀](#)[▶](#)[Back](#)[Close](#)[Full Screen / Esc](#)[Printer-friendly Version](#)[Interactive Discussion](#)

MIPAS retrievals Of
acetylene

R. J. Parker et al.



(a) East-West along 30° N



(b) East-West along 20° N

Fig. 10. Zonal cross-sections of the retrieved C₂H₂ distributions along the 20° N and 30° N lines of latitude, passing through the strong Asian monsoon anticyclone isolation. The NCEP mean tropopause pressure for August 2003 is shown by the red dashed line.

Title Page

Abstract

Introduction

Conclusions

References

Tables

Figures

◀

▶

◀

▶

Back

Close

Full Screen / Esc

Printer-friendly Version

Interactive Discussion



MIPAS retrievals Of acetylene

R. J. Parker et al.

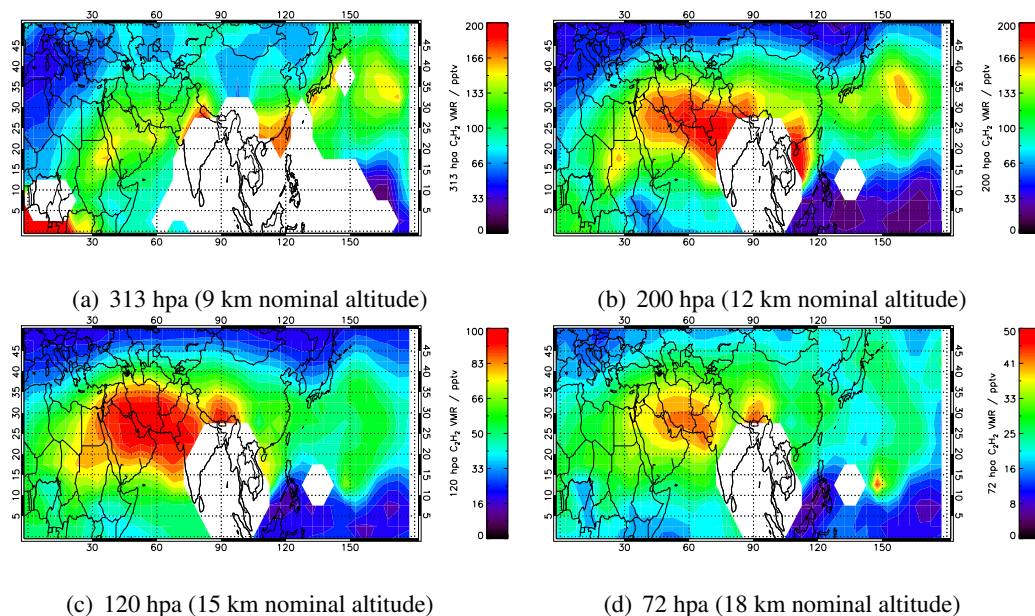


Fig. 11. The MORSE retrieved C_2H_2 distributions for August 2003 located over the Asian monsoon anticyclone region for the 9 km, 12 km, 15 km and 18 km nominal MIPAS tangent altitudes. The strong Asian monsoon anticyclone isolation is clearly evident as well as significant transport from Asia towards North America, particularly at lower altitudes.

Title Page

Abstract

Introduction

Conclusions

References

Tables

Figures

◀

▶

◀

▶

Back

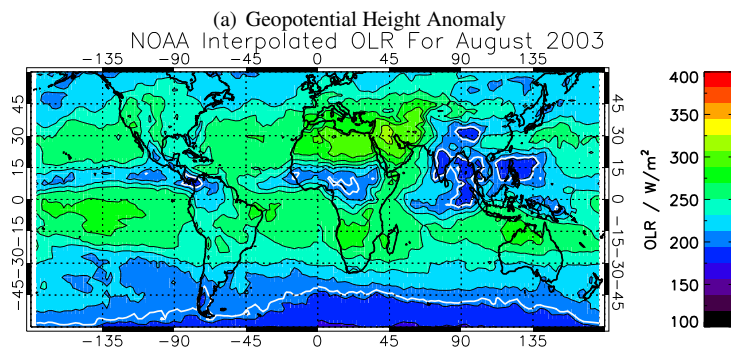
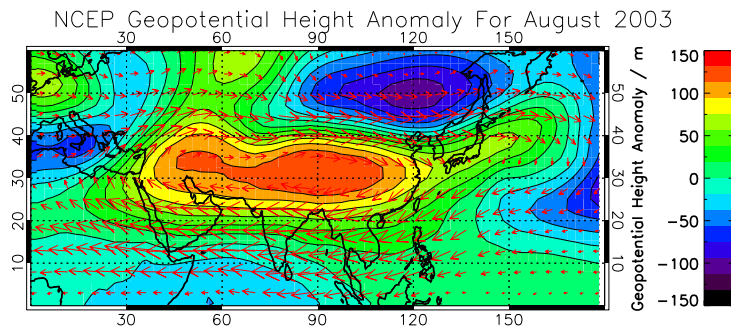
Close

Full Screen / Esc

Printer-friendly Version

Interactive Discussion





(b) OLR

Fig. 12. The Geopotential Height Anomaly and Outgoing Longwave Radiation for August 2003. The geopotential height anomaly is used as an indication for the anticyclone location and is shown to be in strong agreement with the enhanced C_2H_2 chemically isolated by the monsoon anticyclone. The OLR is used to indicate areas of deep convection (i.e. $OLR < 205 W/m^2$) which are outlined by the white contour lines. These show the large area of deep convection over India and South-East Asia, on the South-Eastern edge of the Asian monsoon anticyclone.

MIPAS retrievals Of acetylene

R. J. Parker et al.

Title Page

Abstract Introduction

Conclusions References

Tables Figures

◀ ▶

◀ ▶

Back Close

Full Screen / Esc

Printer-friendly Version

Interactive Discussion



MIPAS retrievals Of acetylene

R. J. Parker et al.

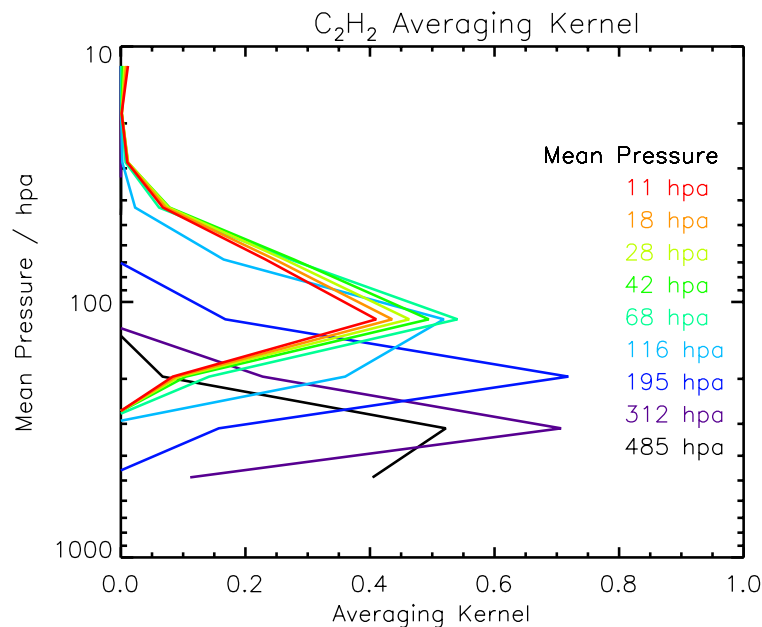


Fig. 13. A example of a typical averaging kernel over the monsoon anticyclone showing the sensitivity of the retrieval at 200 hpa and 300 hpa. Note that there is no discernible C_2H_2 signal above 100 hpa as expected, the C_2H_2 sensitivity is largely confined to the upper troposphere.

[Title Page](#)[Abstract](#)[Introduction](#)[Conclusions](#)[References](#)[Tables](#)[Figures](#)[◀](#)[▶](#)[◀](#)[▶](#)[Back](#)[Close](#)[Full Screen / Esc](#)[Printer-friendly Version](#)[Interactive Discussion](#)